Saddle-point "trapping" of Rydberg electrons in crossed electric and magnetic dc fields: A time-dependent approach

Charlotte Nessmann and William P. Reinhardt
Department of Chemistry/D5, University of Pennsylvania, Philadelphia, Pennsylvania 19104
(Received 2 June 1986; revised manuscript received 29 December 1986)

The possibility of a microscopic Penning trap [suggested by C. W. Clark, E. Korevaar, and M. G. Littman, Phys. Rev. Lett. **54**, 320 (1985)] formed by the magnetic-field-induced stabilization of saddle-point motion of an atomic electron moving in the presence of combined internal Coulomb and externally applied electric and magnetic potentials is investigated using time-dependent methods. Photoeffect spectra are calculated as the Fourier transform of the dipole correlation function for propitiously chosen initial conditions, and these indeed show oscillations as predicted by Clark *et al.* However, it is shown that maximal trapping occurs for the case in which only the magnetic field is present (giving the usual Landau confined states for electrons with zero average mechanical momenta) and that the Stark-Coulomb saddle point simply destabilizes this simpler motion. Both the relationship of the calculated spectra to the propagation of wave packets in the combined fields and their relationship to the periodic classical orbits "quantized" by Clark *et al.* are discussed. The more difficult problem of predicting what might be observed in a photoeffect spectrum of an atomic ground state in the presence of crossed external fields is also discussed from the time-dependent perspective.

I. INTRODUCTION

The effect of an external dc field on near-threshold photoionization and photodetachment cross sections has been a subject of intense interest since the early observations by Garton and Tomkins[1] of magnetic-field-induced oscillations in the photoionization of alkali-metal and alkaline-earth-metal atoms.[2] Subsequent experiments[3] showed that dc electric fields could also induce oscillations in photoionization cross sections, and that photodetachment of negative ions in a dc magnetic field also gave rise to new structures near threshold.[4] Theoretical explanations and models have rapidly developed,[5] as well as quantitative predictive theory for the case of electric field effects where the hydrogenic problem has been directly solved,[6] and for alkali-metal atoms the multi-channel quantum-defect approach of Seaton[7] and Fano[8] has been beautifully developed and applied by Harmin.[9] The magnetic field case is much less well developed from a quantitative theoretical point of view, as the problem of asymptotic motion in a combined Coulomb and (quadratic) Zeeman field is neither separable nor integrable,[10] although substantial regularities are seen in the predicted hydrogenic Zeeman effect below the ionization threshold.[11]

Work on the problem of *combined* E and B fields is beginning to appear.[12] Quite recently Clark, Korevaar, and Littman,[13] referred to as CKL hereafter, have made theoretical predictions of a new type of threshold effect to be expected in combined dc electric and magnetic fields. Specifically, for the case of perpendicular E and B fields the possibility of a microscopic trapping of a Rydberg electron in the vicinity of the Stark-Coulomb saddle point has been proposed, and experiments are under way to determine whether such a trapping might manifest itself in photoionization spectra in such crossed fields.[14] Burkova *et al.*[15] and Bhattacharya and Rau[16] have also suggested novel effects coming from combined E and B fields, but these works consider effects far from the CKL saddle point. Other experimental investigations in combined E and B fields are also underway.[17,18]

It is the purpose of the present paper to give an analysis of the CKL predictions. Using time-dependent wave-packet techniques, we make predictions of spectral features to be expected if specific initial states can be prepared in the laboratory. We will argue (qualitatively) that any such effects will be greatly lessened in more usual experimental situations.

The model of CKL is reviewed in Sec. II, where, in particular, the quadratic approximation of CKL is introduced to describe motion in the saddle-point region. The fundamentals of the time-dependent method are introduced in Sec. III, and applied to the problem of quantum dynamics in the Stark-Coulomb saddle-point region[19] in the absence of the magnetic field. In this case, assuming the quadratic approximation of CKL, the time-dependent Schrödinger equation is exactly soluble for motion of an initially Gaussian wave-packet whose center follows the classical dynamics of the system. Such a solution to the time-dependent Schrödinger equation has been introduced previously by Heller, whose work we follow, and extensively applied to the case of dissociative molecular dynamics.[20] The immediate result of this $B=0$ analysis is that, although there is a one-parameter family of classical bound states in the continuum (just as in the CKL case), no sharp spectral features are to be expected. In Sec. IV, the Heller ansatz is extended to the case of motion in a quadratic saddle-point potential and a perpendicular B field. Again, as in the $B=0$ case, packets whose centers follow the classical dynamics are found, and it is shown in the results presented in Sec. V, that the effect of the B field is not only to determine the precise trajectories of trapped classical orbits, but also to stabilize the spreading

of the quantum wave-packets transverse to the B field. For sufficiently large B fields we begin to see structure appear in the model photoeffect spectra, thus confirming the essential expectations of CKL, but for quite specific initial preparation of the Rydberg electron in the trapping region. However, it is readily apparent that the largest trapping occurs in the limit that the B field completely dominates the Stark-Coulomb potential: that is, the optimum trapping is for Landau levels with zero mechanical momentum. In Sec. VI we use the Wigner-Weyl phase-space correspondence to compare the leading-order semiclassical results for the full potential with the results obtained by the quadratic approximation of the potential mentioned above. Sec VII concludes the paper with a discussion of the possibility of observing saddle-point effects in actual photoeffect spectra, and includes a discussion of the technical theoretical developments needed to carry out a more quantitative analysis.

II. TRAPPED TRAJECTORIES AND THE QUASI-PENNING TRAP

A. The Clark-Korevaar-Littman analysis

CKL have found a one-parameter family of periodic (and thus trapped) orbits near the Stark-Coulomb saddle point, defined below, in the presence of a magnetic field. This has led to the suggestion that a "microscopic" analog of a Penning trap[21] might have been found, with the possibility of a highly localized but long-lived series of electronic states of a new type. The CKL analysis is basically classical, with quantum predictions based on a semiclassical interpretation of the periodic classical orbits. We briefly review the CKL analysis, including the quadratic approximation introduced by them. It is this quadratic approximation of the saddle-point potential which allowed CKL to obtain an analytic expression for the 1:1 periodic orbits[22] and a subsequent expression for the energy levels. In Secs. III and IV it is this same approximation which allows us to carry out exact quantum dynamics, and thus to make explicit predictions of spectral effects.

The motion of a Rydberg electron moving far from an atomic ionic core but subjected to an external dc electric field of strength E in the x direction is determined by the Stark-Coulomb (SC) potential (atomic units, $\hbar=m_e=e^2=1$ are used hereafter)

$$V^{\mathrm{SC}}(x,y,z)=-(x^2+y^2+z^2)^{-1/2}-Ex \ , \tag{2.1}$$

where it is assumed that the nucleus is stationary at $x=y=z=0$. The potential $V^{\mathrm{SC}}(x,0,0)$ has a local maximum at $x_0=E^{-1/2}$ as a function of x, and $V^{\mathrm{SC}}(x,y,z)$ has a saddle point at $x=x_0,y=z=0$ when considered as a function of all three Cartesian variables. It is this electric-field-induced saddle point, far from the nucleus for small to moderate laboratory fields, which we refer to as the Stark-Coulomb saddle point. To include the dc magnetic field (of strength B and directed along the z axis), CKL introduce the Lagrangian

$$L=\tfrac{1}{2}(\dot{x}^2+\dot{y}^2+\dot{z}^2)-V^{\mathrm{SC}}+\frac{\omega_c}{2}(y\dot{x}-x\dot{y}) \ , \tag{2.2}$$

where ω_c is the cyclotron frequency, $\omega_c=B/c$ (note again that the units are a.u.). Direct numerical integration of Lagrange's equations yielded closed orbits around the Stark-Coulomb saddle point. It is the existence of such orbits that suggests localized quantum states. CKL note that the trapped orbits are unstable; a small perturbation of initial conditions leads to rapid drift from the trapping region suggesting that the quantum states will be resonances, rather than bound states in the continuum.

To allow an analytic formula for the predicted quantum levels associated with the trapped orbits, CKL further simplified the problem by assuming that V^{SC} could be replaced by a Taylor expansion about the saddle point $(x_0,0,0)$:

$$V^{\mathrm{QSCA}}(x,y,z)=V_c+\frac{1}{2x_0^3}[z^2+y^2-2(x-x_0)^2] \ , \tag{2.3}$$

where $V_c=V^{\mathrm{SC}}(x_0,0,0)$, and only quadratic terms have been kept. We refer to this as the quadratic Stark-Coulomb approximation (QSCA) in what follows. Use of V^{QSCA} rather than V^{SC} in the Lagrangian of Eq. (2.2) allows separation of the motion into harmonic motion in the z direction (axial) with frequency $\omega_a=E^{3/2}$, and (1:1 harmonic-like) elliptical motion in the xy plane (transverse), with a frequency ω_t given by solution of the quartic equation

$$\omega_t^4+(\omega_a^2-\omega_c^2)\omega_t^2-2\omega_a^4=0 \ . \tag{2.4}$$

CKL verified that the trapped orbits of the QSCA well approximated those of the full dynamics, and then suggested that the corresponding quantum levels would be given by the harmonic ansatz

$$E_{n_t,n_a}=V_c+(n_t+1/2)\omega_t+(n_a+1/2)\omega_a \ , \tag{2.5}$$

n_t and n_a being the transverse and axial quantum numbers. For the fields $E=5000$ V/cm and $B=150$ kG, $\omega_t=13.2\ \mathrm{cm}^{-1}$ and $\omega_a=6.8\ \mathrm{cm}^{-1}$, suggesting experimental observation might be possible, at least in terms of the moderate energy resolution required.

B. Questions raised by the classical-semiclassical analysis

If we uncritically assume the presence of quantum states localized in the vicinity of the Stark-Coulomb saddle point, their observability depends on the width of the resonances and on their effect on the particular photoeffect transition amplitude probed in a particular experiment. If the widths of the resonances are large compared to their spacing, no structure will be evident. This argues strongly for a theoretical analysis which gives the widths as well as the spacings of the resonances. Such a theory is reviewed for the $B=0$ case in Sec. III, and extended to the $B\neq 0$ case in Sec. IV, with the conclusion that it is indeed important to worry about widths of the resonant states.

If observation of the quasi-Penning resonances is to take place a second question is what is the effect of the resonances on the amplitude

$$\langle \phi_{\mathrm{final}} \mid D \mid \phi_{\mathrm{bound}} \rangle \ , \tag{2.6}$$

where $\mid \phi_{\mathrm{bound}} \rangle$ is the initial bound state, D an appropriate transition operator, and $\mid \phi_{\mathrm{final}} \rangle$ the final (unbound) state.

In most experimental situations, the nonstationary state $D\,|\,\phi_{\text{bound}}\rangle$ is highly localized near the nucleus; in fact, this state will be exponentially bounded with a scale size small compared to the distance from the nucleus to the saddle point. Suppose the quasi-Penning states were, as is the case classically, bound states in the continuum[23] and highly localized near the saddle point: what then will be the overlap between the two normalized and localized types of wave functions with centers perhaps far apart compared to the characteristic spatial dimensions of either eigenstate? If, in the actual case, the resonances are sharp, the same question applies; but if they are broad and the states are more delocalized, a larger contribution to the oscillator strength might be made, but the effect of individual resonances will wash out as the resonances broaden. The classical analog of this question would be do trajectories starting near the nucleus, with momenta characteristic of those in the Wigner transform[24] of $D\,|\,\phi_{\text{bound}}\rangle$, ever approximate the harmonic-like trapped orbits of CKL: or, conversely, do the unstable orbits around the Stark-Coulomb saddle point ever pass near the nucleus? Or, does the presence of the B field effectively prevent this? Put more succinctly, the localized states may well exist, but have no observable effect in a photoeffect experiment initiating with the atomic ground state. In Secs. III–V this latter aspect of the potential observability of the quasi-Penning resonances is avoided: it is assumed that an experimentalist can create initial excitations with prespecified properties, in particular to modify either D or $|\,\phi_{\text{bound}}\rangle$ to produce optimal states for observation of saddle-point resonance structure. A brief discussion of the theoretical developments needed to go beyond this, admittedly simplistic, assumption is given in the discussion.

What is the role, if any, of a single periodic orbit of the type found by CKL in predicting energy levels? In what follows[25] it is argued that the content of the periodic orbits lies in their signaling possible quantum "recurrences" (in a time-dependent view of the photoeffect process), which, in turn, imply oscillations in spectra, rather than making predictions of the positions of particular energy levels. Also, unlike the general periodic orbit techniques of Gutzwiller[26] and Berry and Tabor,[27,28] only information concerning that portion of the spectrum relevant to a particular set of initial phase-space conditions is obtained. This is, of course, an advantage provided that the initial conditions are appropriate to those of a particular experiment. The quantization condition of Eq. (2.5) is then interpreted in terms of its ability to mimic the frequencies which are inverse to the return time(s) of a quantum wave packet corresponding to specific initial conditions. The wave-packet method then provides a natural extension of the periodic orbit WKB quantization methods of Edmonds and Starace, and Rau (Ref. 5), in that actual spectral features, rather than only spacings of oscillations are predicted.

III. TIME-DEPENDENT APPROACH TO SPECTRA: SADDLE-POINT MOTION FOR $B=0$

We give a short outline of the time-dependent formulation of the photoabsorption cross section, following Heller,[20] since this time-dependent "semiclassical" approach differs in both philosophy and technique from the usual WKB methods. As is shown below, the spectrum is determined by the Fourier transform of the autocorrelation function $\langle\phi\,|\,\phi(t)\rangle$, where $\phi(t)$ is a Gaussian wave packet (or a combination of Gaussian wave packets). The position and momentum of the center of the wave packet obey the classical Hamilton's equations of motion and thus the spectral features can be described in terms of classical dynamics.

A. Spectra, time correlation functions, and classical motion

Using the usual electric dipole approximation for the electromagnetic wave, we find that the cross section for photoemission is proportional to $\Sigma(\omega)$, the square of the matrix element of the perturbation between the unperturbed states,

$$\Sigma(\omega)=|\,\langle\psi_f\,|\,D\,|\,\chi_{\text{bound}}\rangle\,|^2\,, \tag{3.1}$$

where $\psi_f(E)$ is the energy normalized final state, $E=\omega+E_{\text{bound}}$, E_{bound} and χ_{bound} are the initial bound-state eigenvalue and eigenfunction, and D is the transition dipole operator. If we set

$$|\,\phi\rangle=D\,|\,\chi_{\text{bound}}\rangle$$

and

$$\rho_\phi=|\,\phi\rangle\langle\phi\,|\,,$$

then

$$\Sigma(\omega)=\text{Tr}[\delta(E-H)\rho_\phi]$$
$$=\frac{1}{2\pi}\int e^{iEt}\langle\phi\,|\,\phi(t)\rangle dt\,,$$

where

$$|\,\phi(t)\rangle=e^{-iHt}\,|\,\phi\rangle,\quad |\,\phi\rangle=|\,\phi(0)\rangle\,,$$

and H is the Hamiltonian which generates the final-state eigenfunction $|\,\psi_f(E)\rangle$. The photoabsorption cross section $\sigma(\omega)$, defined by

$$\sigma(\omega)=4\pi^2\alpha a_0^2\omega\Sigma(\omega)\,,$$

where α is the fine-structure constant, a_0 is the Bohr radius, and ω is the frequency of radiation, is thus proportional to the Fourier transform of the time dipole autocorrelation function $\langle\phi\,|\,\phi(t)\rangle$,

$$\sigma(\omega)=2\pi\alpha a_0^2\omega\int dt\,e^{iEt}\langle\phi\,|\,\phi(t)\rangle\,. \tag{3.2}$$

Equation (3.2) expresses the time-independent photoeffect cross section as the Fourier transform of a time-dependent correlation function: why is this of use? First, if only gross spectral features, such as oscillations in the continuum oscillator strength distribution are desired, relatively short time dynamics determine these, and thus use of $\langle\phi\,|\,\phi(t)\rangle$ as a computational tool is highly advantageous. Second, if, as is often the case for short times, the square integrable packet $|\,\phi(t)\rangle$ remains localized, simple classical arguments, such as Ehrenfest's theorem,[29] often suffice to understand its dynamics, and thus spectral

features may be related to classical dynamics. However, it is important to note that such relationships must be understood in the sense of time and frequency transforms, rather than in terms of direct time-independent semiclassical quantization.

The initial decay of the autocorrelation function is associated with the movement of the packet away from its initial location. This first decay time is thus associated with the force on the packet. A steep potential implies rapid motion of the packet, and thus a broad spectrum. This is consistent with the usual reflection principle arguments applied to molecular dissociation.[30] A second time scale is set as $|\phi(t)\rangle$ returns to the vicinity of $|\phi\rangle$, causing a recurrence in $\langle\phi|\phi(t)\rangle$. Such a recurrence at time τ_2 induces oscillations at frequency $2\pi/\tau_2$ in the time-independent frequency spectrum. To the extent that classical dynamics determines this recurrence time, as is often the case, there *is* an association between a classical periodic orbit and spectral features; however, this is a transform relationship, rather than a semiclassical quantization of an individual level. Another time scale in the figure is that of the damping of the sequence of recurrences; it is the reciprocal of this last time scale which determines the width of the spectral oscillations. Intuitively this is related to the instability of the periodic orbit: even though the center of a packet might return to its origin, if the packet has spread too much, no recurrence of any size will appear in $\langle\phi|\phi(t)\rangle$ and thus the spectrum will not show oscillations. This relation of three distinct time scales to three corresponding frequency features is conveniently "summarized in standard Fourier transform relations[31]" and has been developed by Heller[20] in his treatment of the classical dynamics and corresponding spectral features in the photodissociation of polyatomic molecules.

B. Ansatz for the wave packet, classical interpretation

Let us consider now the time evolution of the wave function $\phi(t)$, the dynamics of which will enable us to predict the properties of the cross section. In order to investigate the role of dynamics near the Stark-Coulomb saddle point on photoeffect spectra, we will assume that the initially prepared state $D|\psi_{\text{initial}}\rangle=|\phi(0)\rangle$ is localized near the saddle point, and consider its subsequent propagation. This choice emphasizes the role of the saddle point: if strong spectral features corresponding to the CKL analysis do not arise in this special case, it is doubtful that they will arise at all. Having future applications in mind, we do not use the standard semiclassical techniques (e.g., path-integral techniques[32]), but an alternative approach suggested by Heller.[33] This approach is based on the semiclassical relation between a localized quantum wave packet and the corresponding classical point particle and its equations of motion. The localized wave packet is assumed to be represented by a multivariate Gaussian wave packet, whose center will be seen to move according to the classical equations of motion. An arbitrary $|\phi(0)\rangle$ can be expanded in a linear combination of such states. In two dimensions, for example, the time-dependent Gaussian is described by

$$\begin{aligned}\psi(x,y,t)=\exp i[&\alpha_x(x-x_t)^2+\alpha_y(y-y_t)^2\\&+\lambda(x-x_t)(y-y_t)+p_x(x-x_t)\\&+p_y(y-y_t)+\gamma]\ .\end{aligned}\tag{3.3}$$

Here α_x, α_y, λ, and γ are time-dependent complex variables, x_t, y_t, p_x $[=p_x(t)]$, and p_y $[=p_y(t)]$ are the classical positions and generalized momenta. We require this ansatz for $\psi(x,y,t)$ to fulfill the Schrödinger equation

$$i\frac{d\psi}{dt}=H\psi=(H_0+V)\psi\ ,\tag{3.4}$$

and this condition determines the parameters of $\psi(x,y,t)$ in Eq. (3.3). To evaluate the parameters, we expand V (in the above case V^{QSCA}) up to second order in a Taylor series around the center of the wave packet (x_t,y_t) (which is exact, since the potential is quadratic) and insert the above ansatz for $\psi(x,y,t)$ into the Schrödinger equation (3.3). Comparing like powers of $(x-x_t)$ and $(y-y_t)$ leads to the "equations of motion" of the parameters of the wave function which describe the evolution of the spreading and the shape of the wave packet (see Ref. 33). Thus, the center of the wave packet is evolving according to Hamilton's canonical equations.

If the potential is not quadratic, the potential has to be locally approximated,[33] by which we mean that at every time step the potential is expanded into a Taylor series up to second order in $(x-x_t)$ and $(y-y_t)$. The validity of this local approximation should be examined for each special case. However, as will be seen in the analytical treatment, the system does not have to be separable.

This ansatz can be regarded as a "classical point" moving in phase space, clothed in a Gaussian. The approach is motivated by Ehrenfest's theorem which states that the Hamilton equation hold for the expectation values (see, e.g., Ref. 34)

$$\frac{d}{dt}\langle p\rangle=-\left\langle\frac{\partial H}{\partial x}\right\rangle\ ,\quad\frac{d}{dt}\langle x\rangle=\left\langle\frac{\partial H}{\partial p}\right\rangle\ .\tag{3.5}$$

In the case of a quadratic potential, $H(x,p,t)$ can be replaced by $H(\langle x\rangle,\langle p\rangle,t)$, so that $\langle x\rangle$ and $\langle p\rangle$, the expectation values of the corresponding quantum operators, evolve according to the classical Hamilton's equation and thus follow the classical path for all t.

C. Example: Saddle-point motion for $B=0$

To illustrate our procedure in more detail, we use Heller's ansatz[33] for the saddle-point potential of the combined electric and Coulombic fields around the Stark saddle-point x_0, without the magnetic field. The electron moves back and fourth along the ridge of this saddle-point region, the harmonic motion in z direction is neglected. The potential V is approximated by

$$V^{\text{QSCA}}(x,y)=V_c-\frac{\omega_b^2}{2}x^2+\frac{\omega_a^2}{2}y^2\ ,$$

(see Sec. II), where $V_c=-2\sqrt{E}$ is the classical ionization energy in the presence of the electric field $\omega_a=(x_0)^{3/2}$ and $\omega_b=\omega_a\sqrt{2}$. The potential in the x direction corresponds to an "upside-down" potential, in the y direction it corre-

sponds to a "normal" quadratic potential. In this case the equations of motion of the spreading parameters of the wave packet can be solved analytically. The initial value for γ is chosen so that $\langle\psi(0)\,|\,\psi(0)\rangle=1$; this means that the imaginary part of γ_0 is

$$\mathrm{Im}(\gamma_0)=-\tfrac{1}{4}\ln\left[\frac{4(\mathrm{Im}(\alpha_0)][\mathrm{Im}(\beta_0)]}{\pi^2}\right].$$

Now we have an expression for the wave packet $\psi(t)$ at any time t. The calculation of the time correlation function $\langle\psi\,|\,\psi(t)\rangle$ is straightforward, since $\psi(t)$, initially a Gaussian wave packet, remains Gaussian. Using the relation between the cross section and the Fourier transform of $\langle\psi\,|\,\psi(t)\rangle$, one can predict whether we expect modulations in the threshold photoionization cross sections. Figure 1 shows the evaluation of the wave packet for different initial values for α_x and α_y according to the analytically solved equations for the spreading parameters, where ω_a was chosen 5×10^{-5} in atomic units (this corresponds to $E=1.8\times10^{-6}$ a.u. or 9.26 kV/cm). For λ not equal to zero, the differential equations for the wave packet parameters have been solved numerically, and it is found that the behavior of the wave packet remains practically unchanged. In Fig. 2 the real part of ψ is superposed on the potential according to the trajectory of the wave packet. It can be clearly seen that the wave packet spreads rapidly in the direction of negative slope of the potential for any reasonable choice of initial values. Thus the overlap function falls off sharply and hence the Fourier transform shows no significant features, see Fig. 3. Thus, we do not expect any spectral fine structure (on a frequency scale of ω_a and ω_t) to appear for the $B=0$ case, in spite of the existence of periodic classical orbits: the quasi-Penning resonances have widths broad compared to their spacings.

IV. SADDLE-POINT SPECTRUM FOR $B\neq0$; A GENERALIZATION OF HELLER'S ANSATZ

In the quadratic Stark-Coulomb approximation the classical Lagrangian for an electron moving in the quasi-Penning trap is given by

$$L^{\mathrm{QSCA}}=\tfrac{1}{2}\dot{x}^2+\tfrac{1}{2}\dot{y}^2+\tfrac{1}{2}\dot{z}^2-V_c-\frac{1}{2x_0^3}(z^2+y^2-2x^2)+\frac{\omega_c}{2}(y\dot{x}-x\dot{y}),$$

where ω_c is the cyclotron frequency (see Sec. II A). For this approximation of the potential, the equations of motion for the electron can be solved analytically.

Since the motion along the z axis is harmonic, we neglect it and consider only the motion in the xy plane. Thus, we take the two-dimensional Gaussian of Eq. (3.3) as ansatz for the wave packet ψ, where p_x and p_y denote the generalized momenta, in order to get consistency with the corresponding quantum Hamiltonian. ψ must satisfy the Schrödinger equation and this condition determines the time-dependent parameters α_x, α_y, λ, and γ. If we choose the vector potential **A** so that **p** and **A** commute, we obtain the Hamiltonian

$$\begin{aligned}H=&-\frac{1}{2}\frac{\partial^2}{\partial x^2}+i\frac{\omega_c}{2}y\frac{\partial}{\partial x}+\frac{\omega_c^2}{8}y^2\\&-\frac{1}{2}\frac{\partial^2}{\partial y^2}-i\frac{\omega_c}{2}x\frac{\partial}{\partial y}+\frac{\omega_c^2}{8}x^2\\&+V_0+V_x(x-x_t)+V_y(y-y_t)+\tfrac{1}{2}V_{xx}(x-x_t)^2\\&+\tfrac{1}{2}V_{yy}(y-y_t)^2+V_{xy}(x-x_t)(y-y_t)\,.\end{aligned}\tag{4.1}$$

We insert Eqs. (3.3) and (4.1) into the Schrödinger equation (3.4), and comparing coefficients of like powers of x and y [the symmetry around the center of the wave packet (x_t,y_t) has been lost], we find the equations of motion for the "spreading parameters" of $\psi(x,y,t)$:

$$\alpha_x=-2\alpha_x^2-\frac{\lambda^2}{2}-\frac{\omega_c}{2}\lambda-\frac{1}{2}V_{xx}-\frac{\omega_c^2}{8}\,,\tag{4.2a}$$

$$\alpha_y=-2\alpha_y^2-\frac{\lambda^2}{2}+\frac{\omega_c}{2}\lambda-\frac{1}{2}V_{yy}-\frac{\omega_c^2}{8}\,,\tag{4.2b}$$

$$\dot{\lambda}=-2\lambda(\alpha_x+\alpha_y)+\omega_c(\alpha_x-\alpha_y)-V_{xy}\,,\tag{4.2c}$$

$$\dot{\gamma}=i(\alpha_x+\alpha_y)-E+p_x\dot{x}_t+p_y\dot{y}_t\,,\tag{4.2d}$$

where

$$E=V_0+\tfrac{1}{2}\dot{x}_t^2+\tfrac{1}{2}\dot{y}_t^2\,,$$

$$p_x=\dot{x}_t+\frac{\omega_c}{2}y_t\,,$$

$$p_y=\dot{y}_t-\frac{\omega_c}{2}x_t\,.$$

Note that $\dot{\pi}_x=-\omega_c\pi_y-V_x$ and $\dot{\pi}_y=\omega_c\pi_x-V_y$, where π_x, π_y denote the mechanical momenta $\dot{x}_t,\dot{y}_t$. The last three terms in (4.2d) are recognized as the action integral along the classical trajectory. Note that the equations for $B=0$ are a special case of the above ones.

To evaluate the propagation of the wave packet, we solve Eqs. (4.2a)–(4.2d) and insert the results into the equation for the wave function (3.3). In general this is achieved only with the assistance of numerical methods. If, however, $B=0$, then the potential corresponds to a "saddle-point region" potential, with one normal harmonic oscillator potential in the y direction and an upside-down harmonic oscillator potential in the x direction, and the equations of motion of the spreading parameters can be solved analytically (see Sec. III). Similarly, if we consider *only* the magnetic field B and assume further that $\lambda(t=0)=(0,0)$ and $\alpha_x(t=0)=\alpha_y(t=0)$, so that the wave packet is uncoupled in the x and y directions, then the wave-packet propagation is equivalent to the Hamiltonian of a two-dimensional harmonic oscillator and the equations for the evolution of the wave packet are well known (see Sec. V B). From the time-dependent wave packets the time correlation function can be evaluated and the subsequent Fourier transform (usually via fast-Fourier-transform routines) leads to the absorption spectrum according to Eq. (3.2).

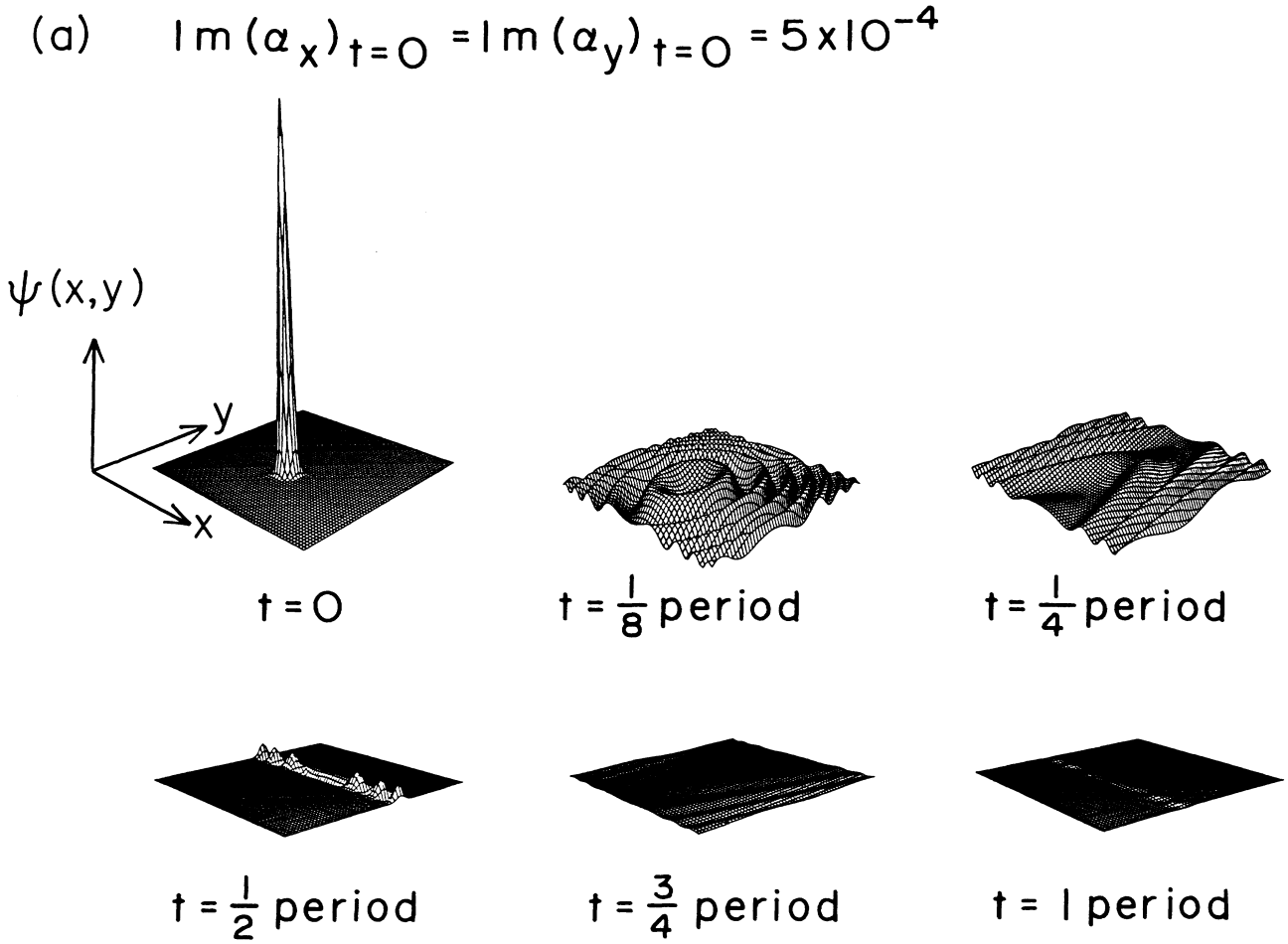

FIG. 1. Evaluation of the real part of the wave packet for different initial values of α_x,α_y. The wave packets are evolving under the influence of the combined electric and Coulomb field which has been harmonically approximated. $\omega_a = 5\times10^{-5}$ in atomic units (this corresponds to $E = 9.26$ kV/cm). The wave function has initial values $\lambda = (0,0)$ and $\mathrm{Re}(\alpha_x) = \mathrm{Re}(\alpha_y) = 0$; $\mathrm{Im}(\alpha_x) = \mathrm{Im}(\alpha_y) = 5\times10^{-4}$ and $\mathrm{Im}(\alpha_y) = 5\times10^{-6}$ for Fig. (a) and (b), respectively.

V. NUMERICAL RESULTS

A. General case

We encountered some numerical difficulties because the three coupled, complex-valued differential equations (4.2a)—(4.2c) were too stiff for the most commonly used differential-equation-solver routines. We found that ATOMCC[35] was most successful under these conditions. The numerical accuracy depends on the choice of the initial wave-packet parameters and the choice of the electric and magnetic field. In what follows, the parameters are such that no numerical problems arise.

The electric field was taken to be 10^{-6} a.u. (which is 5142 V/cm), so that the Stark saddle point x_0 is in a distance of 1000 a.u. from the atomic nucleus. The magnetic field was varied between 1.5×10^3 and 1.5×10^6 G. Unless mentioned otherwise, the initial values of $\mathrm{Im}(\alpha_x)$ and $\mathrm{Im}(\alpha_y)$ were chosen in such a way that the magnitude of the wave packet at the classical trajectory corresponding to the next higher transversal quantum number (see Ref. 13) has decreased to $1/e$ times the maximum value of the wave packet.

Guided by the results for $B = 0$ (see Sec. III) one might expect that the spreading still prevents any significant recurrence of the autocorrelation function after one period. This is the case if the magnetic field is not too strong: for example, $B = 1.5\times10^3$ G. In this case the wave packet spreads along the ridge of the saddle-point region and already after half a period resembles a plane wave. No recurrence can be found in the overlap function.

For $B = 1.5\times10^4$ G the main features remain the same, that is a quick spreading in the direction of negative slope of the potential, but the "plane" wave packet no longer points in the same direction. The orientation of the wave packet depends on the initial values of position and momentum of the wave packet. In the same way, the spreading parameters show some equilibration which depends on the initial conditions.

Assuming an even stronger magnetic field, e.g., $B = 1.5\times10^5$ G, the magnetic cyclotron frequency ω_c becomes comparable to ω_t, the recurrence frequency of the

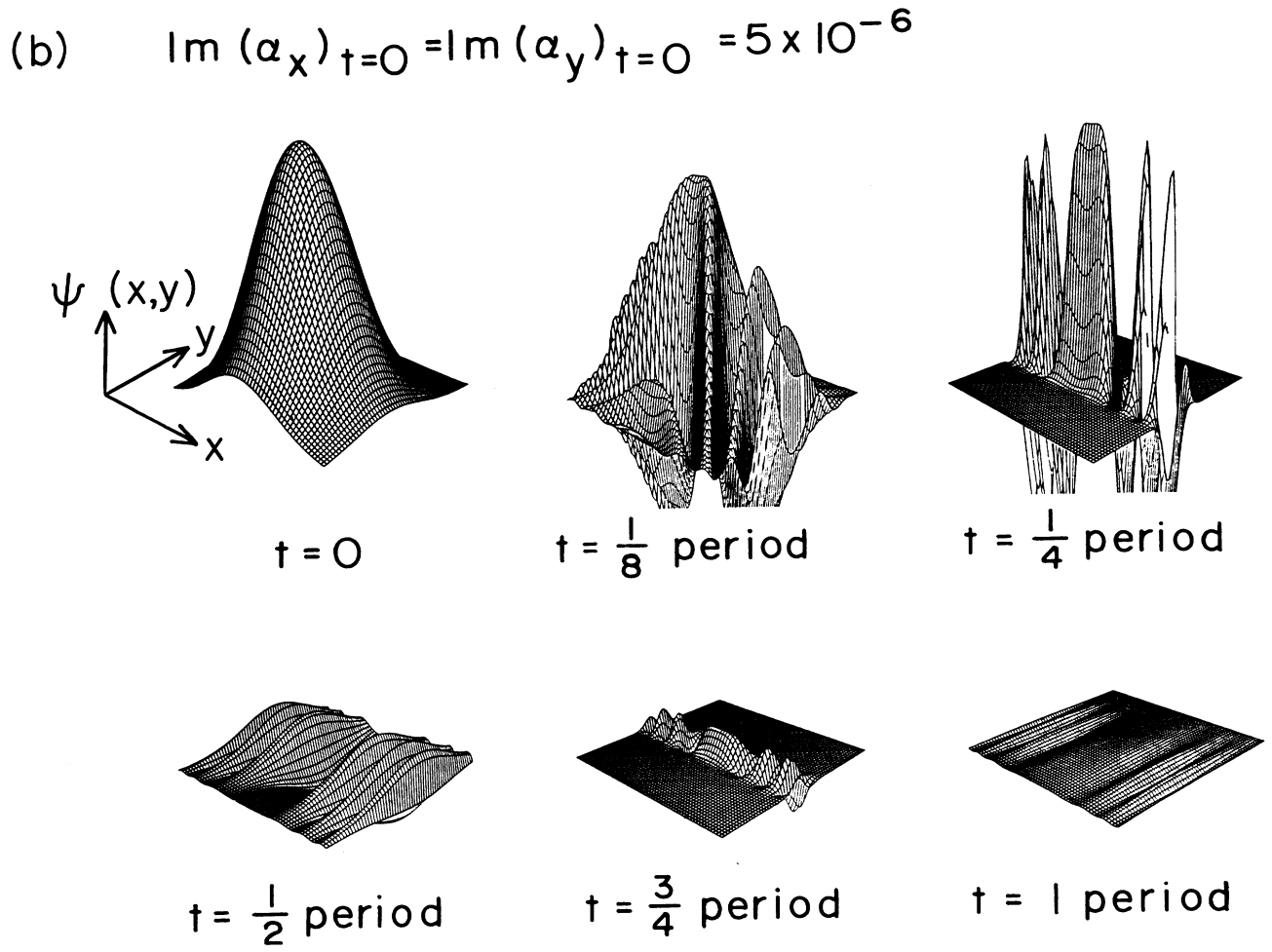

FIG. 1. (*Continued*).

periodic orbit. Though there is still spreading in the declining part of the saddle-point region, the dynamics of the spreading parameters becomes more and more important. The Lorentz force drives back the spreading part of the wave packet to the ascending part of the potential, thus causing a confinement of the wave packet. But, as can be seen in Fig. 4, the wave packet is still expanded so much that it will not pass over the barrier of the potential and so will maintain its orientation after a half period. Figure 5 shows the time correlation functions and their Fourier transforms for $B=1.5\times10^4$, 1.5×10^5, and 1.5×10^6 G. They indicate clearly the effects of spreading and confinement on the features of the spectra. The overall envelope of the peak in the Fourier transforms is determined by the decay of the autocorrelation function (and thus also determined by the initial values of α_x and α_y). The repetitive overlaps control the onset of peaks and troughs, whose spacing is given by $\omega_t=2\pi/T$, where T is the period of the semiclassical orbit ($\omega_t=3.19\times10^{-5}$, 6.02×10^{-5}, and 6.37×10^{-4} a.u. for the given field strengths). The more slowly the heights of the recurrences in the overlap decay, the sharper become the lines in the spectrum.

For $B=1.5\times10^6$ G one observes the onset of Landau resonances. This implies that the magnetic field is so strong compared to the electric and Coulombic field that it dominates the behavior of the evolution of the wave packet. The spreading becomes negligible and the wave packet retains its shape after one periodic orbit: this indicates that the trapping of the electron is due to the magnetic field and not to the saddle-point potential surface of the combined electric and Coulombic field (which presents a perturbation of the magnetic field).

We find that for magnetic fields of the order of 10^6 G and higher, the problems of numerical accuracy become crucial. Small errors in the evaluation of the spreading parameters result in the displacement of the maximum value of the calculated wave packet from its center (which by construction is pinned down to the semiclassical orbit).

B. Free motion in a uniform magnetic field

If we set $V^{SC}=0$, the wave packet evolves under the effect of a uniform magnetic field along the z axis. The motion in the z direction will again be neglected.

Using the well known result that the motion of the wave packet corresponds to the motion of a wave packet

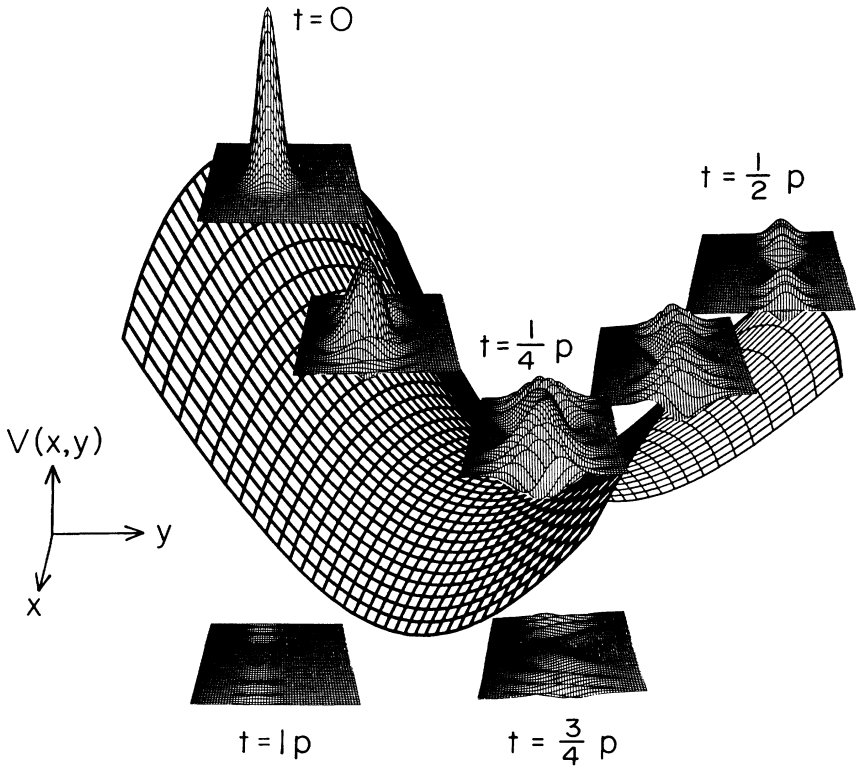

FIG. 2. Wave packet moving along the saddle-point region which is determined by the (approximated) combined electric and Coulombic field. The real part of the wave function is shown during the first period. $E=9.26$ kV/cm, $B=0$. The packet is shown at $t=0$, $\frac{1}{8}$, $\frac{1}{4}$, $\frac{3}{8}$, $\frac{1}{2}$, $\frac{3}{4}$, and 1 of a full period, the latter two are shown *below* the potential surface for clarity.

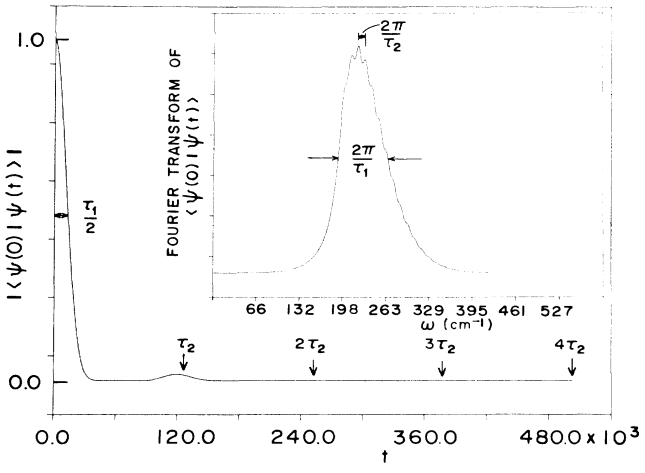

FIG. 3. Autocorrelation function (during the first four periods) and its Fourier transform for the wave packet of Fig. 2. τ_1 indicates the initial decay time and τ_2 the recurrence time in atomic units. The corresponding frequency spacing in the Fourier transform is $2\pi/\tau_2$ (5×10^{-5} a.u. ≈ 10.97 cm^{-1} in the above case), the width of the overall envelope is determined by $2\pi/\tau_1$. The sharper the falloff of the original overlap, the broader becomes the shape of the overall peak in the Fourier transform.

according to the Hamiltonian of a two-dimensional oscillator, and taking $\lambda=(0,0)$ and $\alpha_x=\alpha_y$ in Eqs. (4.2a)–(4.2d), the equations of motion for the spreading parameters can be solved analytically. One gets the same expression as in Sec. III, where ω_a has to be replaced by $\omega_c/2$, both for α_x and α_y. The equation for γ reduces to $\dot{\gamma}(t)=2i\alpha_x$. It is a nice exercise in this case to verify that—disregarding some constant factor—the wave function evaluated according to the above method and the wave function calculated by the well-known path-integral techniques[36] agree exactly. Note that for the special initial values for α_x and α_y, $\alpha_x(t=0)=i\omega_c/4$ and $\alpha_y(t=0)=i\omega_c/4$, the wave packet does not change its shape and is called a Glauber coherent state.[37] The Fourier transform of the autocorrelation function obtained by numerical integration then shows evenly spaced Landau peaks in $\omega_c/2$.

VI. WIGNER-WEYL FORMALISM. COMPARISON WITH APPROXIMATE RESULTS FOR THE FULL POTENTIAL

The analysis of Secs. III–V uses exact quantum propagation within the context of the quadratic approximation to the potential at the Stark-Coulomb saddle point. Since a full treatment of the propagation in the Coulomb poten-

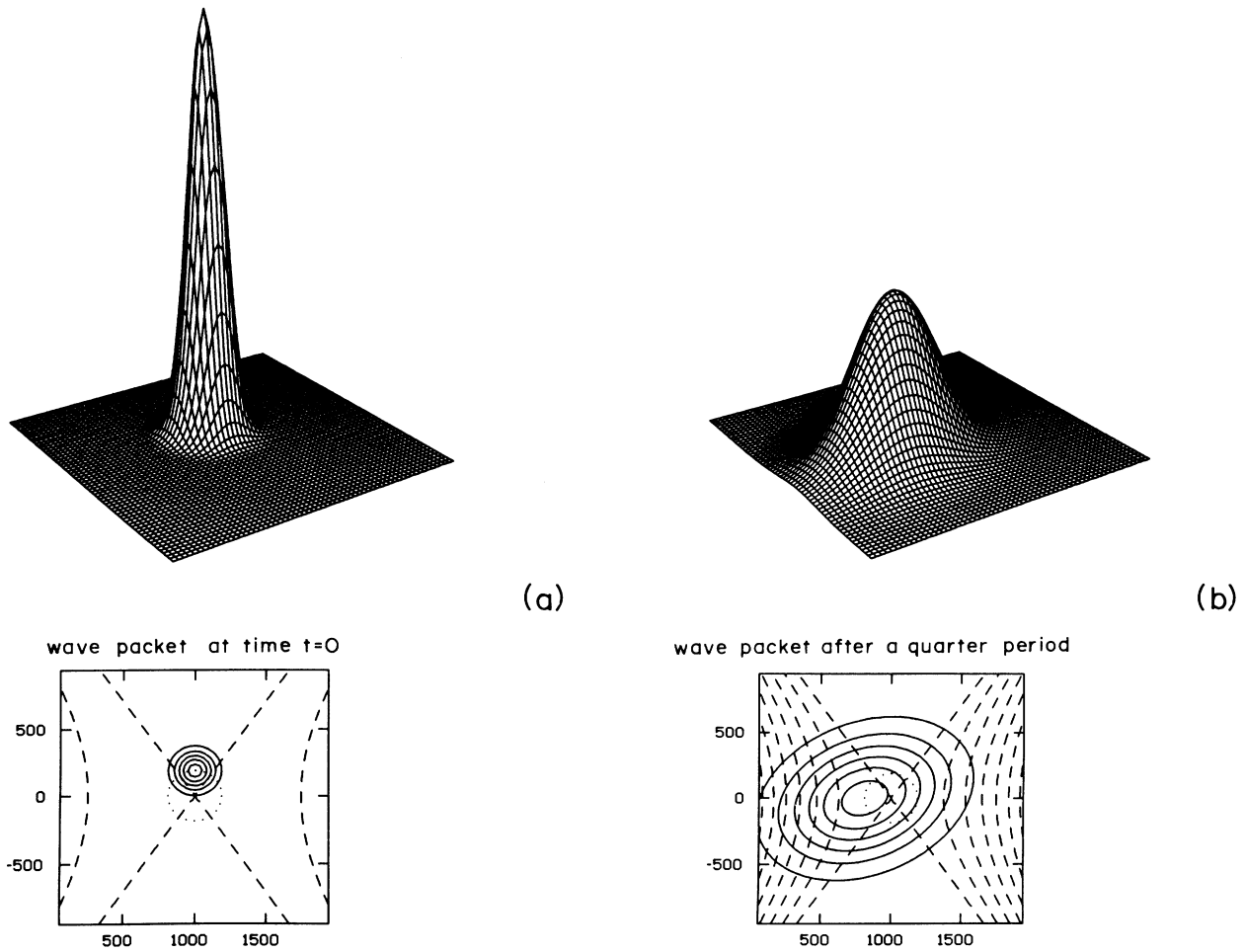

FIG. 4. Evolution of the wave packet for a magnetic field $B=1.5\times10^5$ G along the z axis, and in the Stark-Coulomb potential. The dashed line in the lower part shows the potential-energy surface for the quadratically approximated combined electric and Coulomb field, $E=5142$ V/cm ($=10^{-6}$ in a.u.) along the x axis. The dotted line indicates the trajectory around the saddle point for the lowest resonance. The atomic nucleus is at $x=y=0$ and the Stark saddle point x_0 lies at (1000), measured in atomic units. The scale factor for the height of the wave packet is constant for (a)—(e).

tial is extremely difficult, we apply an approximate procedure to determine the propagation, but for the full potential, and compare the thus derived results with the previous ones.

To this end we make use of the Wigner-Weyl correspondence in phase space. In this formulation of quantum mechanics a quantum state represented by a density operator ρ is given by the Wigner distribution function

$$P_W(\mathbf{q},\mathbf{p})=(\pi)^{-n}\int d^n s\, e^{2i\mathbf{p}\cdot\mathbf{s}}\langle \mathbf{q}-\mathbf{s}\,|\,\rho\,|\,\mathbf{q}+\mathbf{s}\rangle\ . \quad (6.1)$$

In the case of a pure state ψ this can be substituted by

$$P_W(\mathbf{q},\mathbf{p})=(\pi)^{-n}\int d^n s\, e^{2i\mathbf{p}\cdot\mathbf{s}}\psi^*(\mathbf{q}+\mathbf{s})\psi(\mathbf{q}-\mathbf{s})\ .$$

The properties for the Wigner distribution function are commonly known,[38] so we will recall only those we will need in the following. The classical function corresponding to the quantum operator A is thus given by

$$A_W(\mathbf{q},\mathbf{p})=2^n\int d^n s\, e^{2i\mathbf{p}\cdot\mathbf{s}}\langle \mathbf{q}-\mathbf{s}\,|\,A\,|\,\mathbf{q}+\mathbf{s}\rangle$$

and

$$\int d^n q\, d^n p\, A_W(\mathbf{q},\mathbf{p})B_W(\mathbf{q},\mathbf{p})=(2\pi)^n\mathrm{Tr}(AB)\ .$$

The expectation value of the quantum operator A in the state represented by ρ is

$$\langle A\rangle=\mathrm{Tr}(\rho A)$$

and thus

$$\langle A\rangle=\int d^n q\, d^n p\, A_W(\mathbf{q},\mathbf{p})P_W(\mathbf{q},\mathbf{p}) \quad (6.2)$$

by the above expression. The Wigner distribution function evolves in time according to the quantum Liouville equation

$$\frac{\partial P_W}{\partial t}=i[P_W(\mathbf{q},\mathbf{p})e^{\Lambda/2i}H_W(\mathbf{q},\mathbf{p})-H(\mathbf{q},\mathbf{p})e^{\Lambda/2i}P_W(\mathbf{q},\mathbf{p})]\ , \quad (6.3)$$

where H_W is the function corresponding to the Hamilton operator H and Λ is the Janus operator

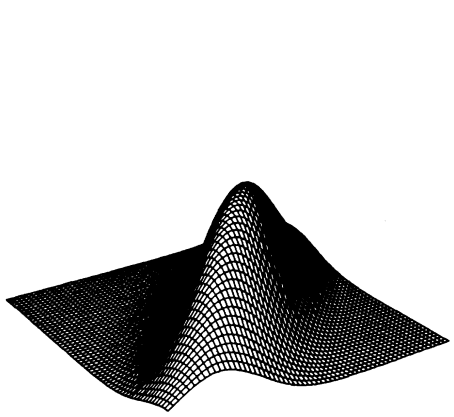

(c)

wave packet after a half period

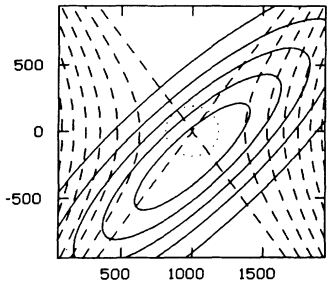

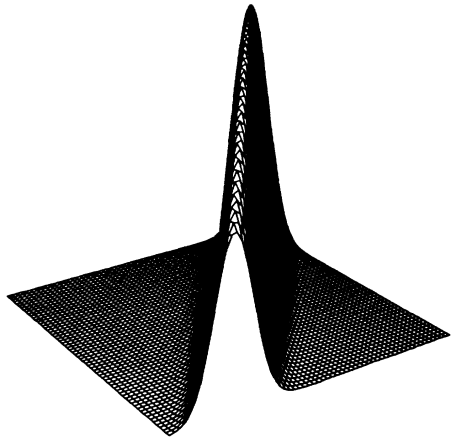

(d)

wave packet after three quarters of a period

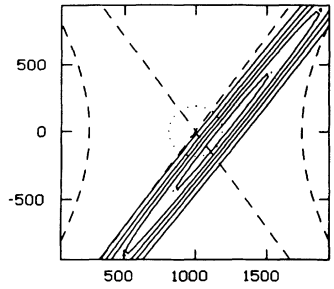

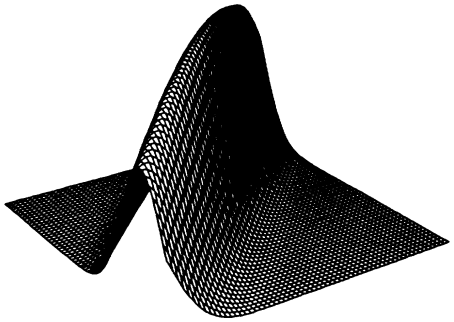

(e)

wave packet after one period

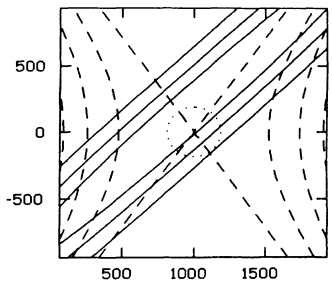

FIG. 4. (*Continued*).

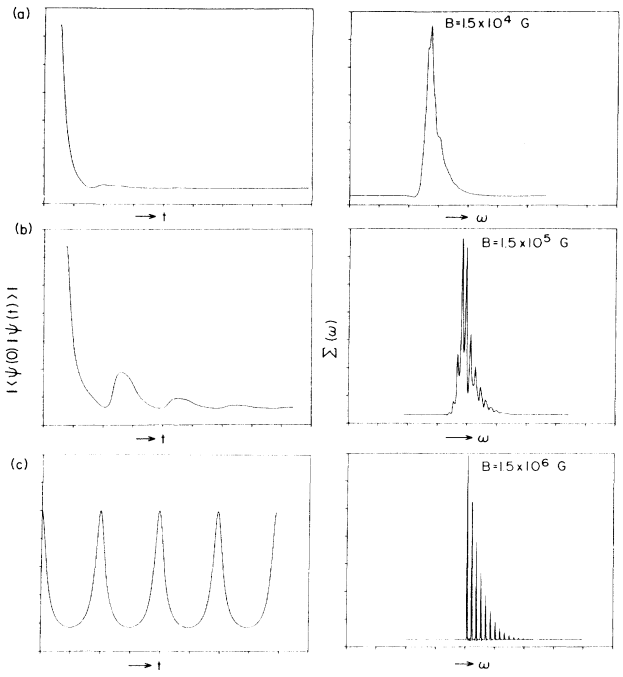

FIG. 5. Autocorrelation functions and their Fourier transforms for various magnetic fields in the presence of the Stark-Coulomb saddle point for $E=5142$ V/cm. The left side shows the autocorrelation function during the first four periodic orbits around the saddle point x_0. The combined electric and Coulombic field is harmonically approximated. The magnetic field B along the z axis varies: (a) 1.5×10^4 G, (b) 1.5×10^5 G, (c) 1.5×10^6 G. The right side shows the corresponding Fourier transforms. The corresponding spacings are (a) 3.19×10^{-5} a.u. or 7 cm^{-1}, (b) 6.02×10^{-5} a.u. or 13.2 cm^{-1}, (c) 6.37×10^{-4} a.u. or 139.8 cm^{-1}. Note that the frequency units for the Fourier transform in (c) have been changed by a factor of 10 compared to the other transforms.

$$\Lambda=\frac{\overleftarrow{\partial}}{\partial p}\frac{\overrightarrow{\partial}}{\partial q}-\frac{\overleftarrow{\partial}}{\partial q}\frac{\overrightarrow{\partial}}{\partial p}\ ,$$

the arrows indicating the directions in which the derivatives have to be taken.

To calculate the photoabsorption cross section [Eq. (3.2)] we are interested in the expression $\langle\phi\,|\,\phi(t)\rangle$ and use

$$|\langle\phi(0)\,|\,\phi(t)\rangle|^2=\mathrm{Tr}(\rho_0\rho_t)\ ,$$

where ρ_0 and ρ_t are the appropriate density operators. According to Eq. (6.2) we can rewrite this expression as

$$|\langle\phi(0)\,|\,\phi(t)\rangle|^2=(2\pi)^n\int d^nq\,d^np\,P_W(\mathbf{q},\mathbf{p},0)\times P_W(\mathbf{q},\mathbf{p},t)\ , \qquad (6.4)$$

where the time evolution of the corresponding Wigner function $P_W(\mathbf{q},\mathbf{p},t)$ is governed by Eq. (6.3).

We introduce here the first approximative step, namely, the substitution of the quantum Liouville propagation by the classical Liouville propagation for density functions. This is exact if the potential does not have any derivatives of order 3 or higher.[39] However, Heller, in a series of papers,[40] argues that this substitution gives reasonable results so long as the Wigner functions correspond to well localized wave packets, or, more precisely, so long as either the initial wave packet or the time evolved wave packet is localized.

For the initial wave packet we choose the "former" Gaussian. If we approximate its corresponding Wigner function by a sum of weighted delta distributions,[40] then the time-evolved Wigner function is easily calculated, i.e.,

$$P_W(\mathbf{q},\mathbf{p},t)=\sum_i\alpha_j\delta(\mathbf{q}-\mathbf{q}_j(t))\delta(\mathbf{p}-\mathbf{p}_j(t))\ ,$$

where the $\mathbf{q}_j(t)$ and $\mathbf{p}_j(t)$ are determined by Hamilton's equations of motion. The use of this approximative expression for the time-evolved Wigner function and the one obtained by the original Gaussian wave packet for the initial Wigner function, makes the evaluation of the phase-space trace (6.4) elementary.

Typical results for the evolution of $P_W(\mathbf{q},\mathbf{p},t)$ in the presence of the full potential are shown in Fig. 6 and compared with the evolution of the same initial Wigner distribution function, but in the quadratically approximated potential (the projection onto the xy plane is shown). It is clear that the long-time behavior differs considerably over the full extent of the packet. But since we are only interested in an overall picture of the photoabsorption cross section, e.g., at resolution $\approx 2\pi/\tau_2$, τ_2 being the first packet recurrence time (see Sec. III), we need only to be concerned about the short time (e.g., $t\approx\tau_2$) features of the wave packet. Additionally, we only need to be concerned with that part which overlaps the initial packet. To calculate $\Sigma(\omega)$ of Eq. (3.1) one needs also the time evolution of the phase of the autocorrelation function. This missing information can be recovered from the amplitude,[41] so that knowing the phase-space evolution of the Wigner distribution functions is sufficient to determine the photoabsorption cross section.

Figure 7 shows the modulus of the autocorrelation function both in the case of the evolution of the Wigner function in the full potential—within our framework of a zero-order approximation to the quantum Liouville equation—and in the case of the quadratically approximated potential as described in the previous sections. The results agree nicely and furthermore, the features also agree with the results from the quantum propagation of the wave packet in the quadratically approximated Stark-Coulomb potential as introduced by Clark *et al.*[13] [compare Fig. 5(b)]. Thus, over the time scale (within the level of resolution) we are interested in, making the quadratic approximation to the Stark-Coulomb potential does not effect the results for the photoabsorption cross section.

VII. DISCUSSION

We have considered the spectrum obtained if a facile experimentalist could create an initial quantum wave packet in the combination of magnetic and electric potentials arising at the Stark-Coulomb saddle point of a Rydberg atom in dc electric and magnetic fields. We have chosen this form of the wave packet for analytic convenience, and because its center follows the classical trajec-

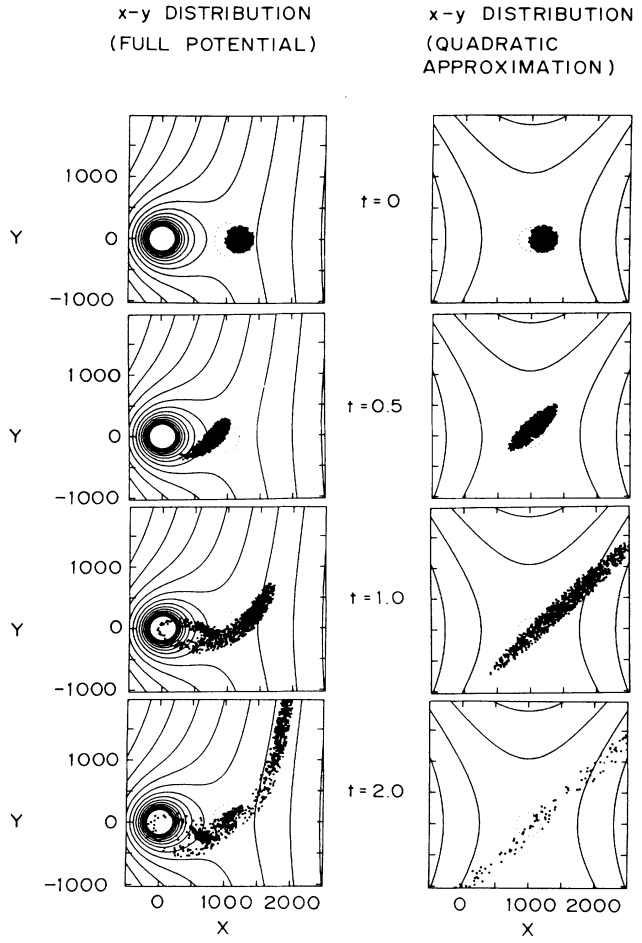

FIG. 6. Evolution of the Wigner distribution function for the full potential and for the quadratically approximated Stark-Coulomb potential. Equipotential contour lines for the Stark-Coulomb potential are indicated by solid lines. The magnetic field $B=1.5\times10^5$ G in both cases, $E=5142$ V/cm. The distribution function is approximated by a sum of 1000 trajectory points in phase space, their projection onto the coordinate space is shown for $t=0$, $t=\frac{1}{2}$ period, $t=1$ period, and $t=2$ periods. The dotted line indicates the (unstable) periodic orbit for $n_t=0$ according to CKL.

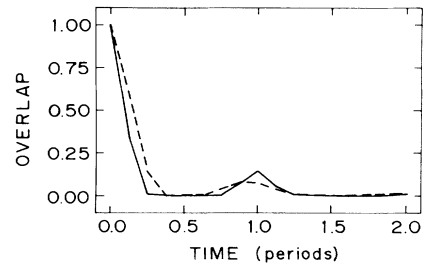

FIG. 7. Modulus of the autocorrelation function of the classical time evolution of a Wigner distribution function in the full potential (solid line) and in the quadratically approximated Stark-Coulomb potential (dashed line). $B=1.5\times10^5$ G and $E=5142$ V/cm; compare with overlap function of the quantum propagation of a wave packet in the quadratically approximated potential shown in Fig. 5(b).

tories found and "quantized" by Clark, Korevaar, and Littman.[13] This latter property of the Gaussian ansatz used allows contact to be made with the predictions of these authors that quasi-Penning trapping might occur. The analytic and numerical results of Sec. V indicate that spectral features are expected with oscillations at frequencies as predicted by CKL. However, rapid transverse spreading of the initially localized packet corresponds to the fact that the quasi-Penning resonances will be quite broad for physically obtainable laboratory fields, and that the optimal trapping occurs for the ordinary Landau levels in a pure B field: the Stark-Coulomb saddle point simply destabilizes this simple motion. Comparison with approximate results for the full potential (within the Wigner-Weyl formalism) presents evidence that making the quadratic approximation to the Stark-Coulomb potential does not effect these conclusions.

In addition to these specific predictions, the role of low-order periodic orbits in determining spectral features is clarified: such periodic orbits should not be used to quantize specific levels, but, if of sufficient stability, may be used to predict gross oscillatory features of the continuous spectrum, or the corresponding modulations of higher resolution discrete spectra.[42] The instability of the orbits correlates with the widths of expected features.

What is the relation of the above analysis to usual photoeffect spectra, where the initial wave packet is $D\,|\chi_{\text{bound}}\rangle$, with D being the usual dipole operator and $|\chi_{\text{bound}}\rangle$ the actual, highly localized atomic ground state? From the point of view adopted here, the answer to this question depends on the existence of trajectories which might "guide" the initial nonstationary state $D\,|\chi_{\text{bound}}\rangle$ from the vicinity of the atomic nucleus to the saddle point and back, on a time scale short compared to the spreading of the packet.

In this respect the "figure-8" trajectories, which Korevaar and Littman[43] calculated, are of special interest. These trajectories cross the region of the atomic nucleus, so that an overlap of the initial bound state, multiplied by the transition operator, and a wave function which corresponds to a figure-8 trajectory might directly take place. In this case one might find spectra with shapes similar to the ones we have shown (Fig.5). However, the spacing between the different peaks in the spectra is $2\pi/T$, where T is the recurrence time of $\psi(t)$ of one closed orbit (see Sec. II), and, therefore, the dynamics of the figure-8 trajectories define the spacing (and their instability the width) of the peaks in the spectra.

ACKNOWLEDGMENTS

One of the authors (C.N.) would like to thank S. J. Singer and Elaine Chandler for helpful conversations. C. N. also wishes to acknowledge the support of the Austrian Fonds zur Förderung der wissenschaftlichen Forschung. This work was also supported by the National Science Foundation through Grant No. CHE84-16459. We thank M. Littman and E. Korevaar for providing us with figures and for interesting conversations throughout the work on this paper.

[1]W. R. S. Garton and F. S. Tomkins, Astrophys. J. **158**, 839 (1969).

[2]W. R. S. Garton, F. S. Tomkins, and H. M. Crosswhite, Proc. R. Soc. London, Ser. A **373**, 189 (1980); N. P. Economou, R. R. Freeman, and P. F. Liao, Phys. Rev. A **18**, 2506 (1978); P. Cacciani, E. Luc-Koenig, J. Pinard, C. Thomas, and S. Liberman, Phys. Rev. Lett. **56**, 1124 (1986). See the reviews of J. C. Gay, in *Progress in Atomic Spectroscopy,* edited by H. J. Beyer and H. Kleinpoppen (Plenum, New York, 1984), Pt. C, p. 177.

[3]R. R. Freeman, N. P. Economou, G. C. Bjorklund, and K. T. Lu, Phys. Rev. Lett. **41**, 1463 (1978); R. R. Freeman and N. P. Economou, Phys. Rev. A **20**, 2356 (1979); T. S. Luk, L. DiMauro, T. Bergeman, and H. Metcalf, Phys. Rev. Lett. **47**, 83 (1981); H. Rottke and K. H. Welge, Phys. Rev. A **33**, 301 (1986).

[4]A. M. Blumberg, W. M. Itano, and D. J. Larson, Phys. Rev. A **19**, 139 (1979).

[5]A. R. Edmonds, J. Phys. (Paris) Colloq. **31**, C4 (1970); A. F. Starace, J. Phys. B **6**, 585 (1973); A. R. P. Rau, Phys. Rev. A **16**, 613 (1977); J. Phys. B **12**, L193 (1979); J. C. Gay, Comments At. Mol. Phys. **9**, 97 (1980); R. J. Fonck, F. L. Roesler, D. H. Tracy, and F. S. Tomkins, Phys. Rev. A **21**, 861 (1980); C. W. Clark and K. T. Taylor, Nature **292**, 437 (1981); J. A. C. Gallas and R. F. O'Conell, J. Phys. B **15**, L309 (1982); W. P. Reinhardt, *ibid.* **16**, L635 (1983); see also the review by C. W. Clark, K. T. Lu, and A. F. Starace, in *Progress in Atomic Spectroscopy,* edited by H. J. Beyer and H. Kleinpoppen (Plenum, New York, 1984), Pt. C, p. 247.

[6]E. Luc-Koenig and A. Bachelier, J. Phys. B **13**, 1743 (1980); **13**, 1769 (1980).

[7]A comprehensive review has appeared, see M. J. Seaton, Rep. Prog. Phys. **46**, 167 (1983), and references therein.

[8]For example, U. Fano, Phys. Rev. A **24**, 619 (1983); U. Fano, J. Opt. Soc. Am. **65**, 979 (1975), and references therein.

[9]D. A. Harmin in, for example, Phys. Rev. Lett. **49**, 128 (1982); Phys. Rev. A **25**, 2565 (1982); **30**, 2413 (1984); and in *Atomic Excitation and Recombination in External Fields,* edited by M. H. Nayfeh and C. W. Clark (Gordon and Breach, New York, 1985), p. 39. This latter is referred to as AEREF in what follows.

[10]W. P. Reinhardt and D. Farrelly, J. Phys. (Paris) Colloq. **43**, C2-29 (1982).

[11]M. L. Zimmerman, M. M. Kash, and D. Kleppner, Phys. Rev. Lett. **45**, 1092 (1980).

[12]H. Crosswhite, U. Fano, K. T. Lu, and A. R. P. Rau, Phys. Rev. Lett. **42**, 963 (1979); E. Korevaar and M. G. Littman, J. Phys. B **16**, L437 (1983); B. R. Johnson, K. F. Scheibner, and D. Farrelly, Phys. Rev. Lett. **51**, 2280 (1983); A. A. Belov, A. P. Kazantsev, D. V. Khveshchenko, and V. L. Pokrovsky, J. Phys. B **18**, 4683 (1985); P. Cacciani, E. Luc-Koenig, J. Pinard, C. Thomas, and S. Liberman, Phys. Rev. Lett. **56**, 1467 (1986). See also the discussion in AEREF (Ref. 9).

[13]C. W. Clark, E. Korevaar, and M. G. Littmann, Phys. Rev. Lett. **54**, 320 (1985); E. Korevaar and M. G. Littman, in AEREF (Ref. 9), p. 157.

[14]E. Korevaar and M. G. Littman (private communication).

[15]L. A. Bukova, I. E. Dzyaloshinskii, G. F. Drukarev, and B. S. Monozon, Zh. Eksp. Teor. Fiz. **71**, 526 (1976) [Sov. Phys.—JETP **44**, 276 (1976)].

[16]S. K. Bhattacharya and A. R. P. Rau, Phys. Rev. A **26**, 2315 (1982).

[17]See the discussion in AEREF (Ref. 9).

[18]H. Rottke, A. Holle, and K. H. Welge (private communication).

[19]Potential saddle-point regions have been of interest in other contents. See for example U. Fano, Phys. Rev. A **22**, 2660 (1980); J. Phys. B **13**, L519 (1980); in *Atomic Physics,* edited by I. Lindgren *et al.* (Plenum, New York, 1983), Vol. 8, p. 5.

[20]E. J. Heller, J. Chem. Phys. **68**, 2066 (1978); **68**, 3891 (1978); in *Potential Energy Surfaces and Dynamical Calculations,* edited by D. Truhlar (Plenum, New York, 1981), p. 103.

[21]F. M. Penning, Physica (Utrecht) **3**, 873 (1936); H. G. Dehmelt, Adv. At. Mol. Phys. **3**, 53 (1967); L. S. Brown and G. Gabrielse, Rev. Mod. Phys. **58**, 233 (1986).

[22]CKL only attempted to find trapped saddle-point orbits satisfying the condition $n_t\omega_t = n_a\omega_a$ for $n_t = n_a = 1$, which are thus 1:1 periodic.

[23]See, for example, J. von Neumann and E. Wigner, Z. Phys. **30**, 465 (1929); F. H. Stillinger and D. R. Herrick, Phys. Rev. A **11**, 446 (1975); H. Friedrich and D. Wintgen, *ibid.* **32**, 3231 (1985), contains a recent discussion from a Rydberg-state perspective.

[24]E. J. Heller and M. J. Davis, J. Phys. Chem. **84**, 1999 (1980); E. J. Heller, *ibid.* **68**, 3891 (1978), and references therein.

[25]This view has been introduced earlier: W. P. Reinhardt, Ref. 5, and AEREF (Ref. 9), p. 85.

[26]M. C. Gutzwiller, Physica **5D**, 183 (1982), and references therein.

[27]M. V. Berry and M. Tabor, Proc. R. Soc. London **349**, 101 (1976).

[28]M. V. Berry and M. Tabor, J. Phys. A **10**, 371 (1977)

[29]See, for example, A. Messiah, *Quantum Mechanics* (Wiley, New York, 1961), Vol. 1, p. 216.

[30]See, for example, G. Herzberg, *Spectra of Diatomic Molecules,* Vol. 1 of *Molecular Spectra and Molecular Structure* (Van Nostrand, New York, 1957), pp. 390–393.

[31]D. C. Champenoy, *Fourier Transforms and Their Physical Applications* (Academic, New York, 1973), p. 39.

[32]For example, I. A. Malkin and V. I. Manko, Zh. Eksp. Teor. Fiz, **59**, 1746 (1970) [Sov. Phys.—JETP **32**, 949 (1971)], consider path-integral methods for charged particles in external E and B fields. These techniques did not easily generalize to the cases treated here.

[33]E. J. Heller, J. Chem. Phys. **62**, 1544 (1975)

[34]K. Gottfried, *Fundamentals,* Vol. 1 of *Quantum Mechanics* (Benjamin, New York, 1966), pp. 67 and 68.

[35]Y. F. Yang and G. F. Corliss, computer program ATOMCC.

[36]R. P. Feynman and A. R. Hibbs, *Quantum Mechanics and Path Integrals* (McGraw-Hill, New York, 1965), p. 64 (beware of misprint).

[37]See, for example, W. H. Louisell, *Quantum Statistical Properties of Radiation* (Wiley, New York, 1973).

[38]E. Wigner, Phys. Rev. **40**, 749 (1932); M. Hillery, R. F. O'Connell, M. O. Scully, and E. P. Wigner, Phys. Rep. **106**, 121 (1984).

[39]F. J. Narcowich, Physica **134A**, 193 (1985); J. Math. Phys. **27**, 2502 (1986). In the latter paper the convergence of expansions for solutions to the quantum Liouville equation is discussed.

[40]E. Heller, J. Chem. Phys. **65**, 1289 (1976); **68**, 2066 (1978); R. C. Brown and E. J. Heller, *ibid.* **75**, (1981); E. J. Heller and R. C. Brown, *ibid.* **75**, 1048 (1981).

[41]E. J. Mele, Synth. Methods **9**, 207 (1984).

[42]As this paper was being completed we received a copy of work before publication by J. Main, G. Wiebusch, A. Holle, and K. H. Welge, Phys. Rev. Lett. **57**, 2789 (1986), where a new class of three-dimensional periodic orbits for the hydrogenic Zee-

man problem was found and, based on the wave-packet interpretation of the oscillatory spectral features, was used to explain frequency oscillations. See also A. Holle, G. Wiebusch, J. Main, B. Hager, H. Rottke, and K. H. Welge, Phys. Rev. Lett. **56**, 2594 (1986); M. A. Al-Laithy, P. F. O'Mahony and K. T. Taylor, J. Phys. B (to be published) discuss the quantum analogues of a class of periodic classical orbits for the quadratic Zeeman problem in the irregular region.

[43]E. Korevaar and M. G. Littman in AEREF (see Ref. 13).